Carbohydrate Polymers 79 (2010) 362–372

Contents lists available at ScienceDirect

Carbohydrate Polymers

journal homepage: www.elsevier.com/locate/carbpol

Structural changes in biodegraded lime wood

Carmen-Mihaela Popescu *, Maria-Cristina Popescu, Cornelia Vasile

Romanian Academy "P. Poni" Institute of Macromolecular Chemistry, Department of Physical Chemistry of Polymers, 41A Gr. Ghica Voda Alley, Ro 700487, IASI, Romania

ARTICLE INFO

Article history:
Received 13 July 2009
Received in revised form 10 August 2009
Accepted 13 August 2009
Available online 18 August 2009

Keywords:
Lime wood
Biodegradation
FT-IR spectroscopy
2D IR correlation spectroscopy

ABSTRACT

The changes in structure of lime wood (*Tilia cordata* Mill.) decayed by *Trichoderma viride* Pers. have been investigated by FT-IR and 2D IR correlation spectroscopy. Wood was exposed to fungi for different durations up to 84 days, with decay assessed through mass loss and FT-IR.

A decrease of intensities bands assigned to different vibrations from cellulose and hemicelluloses, with increasing intensities of the bands assigned to C—O vibrations due to formation of oxidized structures was observed; and examined in details using 2D-correlation spectroscopy and the second derivative analysis in the exposure time range of 0–35 days. The formation of reactive species due to oxidation reactions induced by enzymes was evidenced. It has been also established that after longer degradation period oligomers and oxidized structures result, and finally small fragments containing carboxyl or carbonyl groups are formed, which lead to loss of structural integrity of the lime wood.

1. Introduction

Wood consists in three types of polymers – cellulose, hemicelluloses, and lignin – that are strongly intermeshed and chemically bonded by non-covalent forces and by covalent cross-linkages.

Several types of biodegradation have been recognized in wood, viz. fungal decay, bacterial degradation and insect attack. Fungal decay is the most important and widespread type of degradation and is caused by white-, brown- or soft-rot fungi (Eriksson, Blanchette, & Ander, 1990).

Wood-decaying fungi are the most important microorganisms that can colonize and degrade wood (Zabel & Morell, 1992) by attacking cell components using enzymatic and non-enzymatic systems (Goodell & Jellison, 1998; Goodell et al., 1997).

White-, brown- and soft-rot fungi attack wood by their enzymatic systems. These enzymes penetrate the wood cell wall, alter its chemistry and break down the cell-wall polymers into constituents that can be taken up by hyphae. It was been established that the brown-rot fungi selectively decay cell-wall polysaccharides, with limited lignin degradation. The decay system in this type of fungi is based on both non-enzymic (chemical) and enzymic attacks (Eriksson et al., 1990).

The influence of white-rot decay on wood chemistry has been studied by various methods (Eriksson et al., 1990; Martinez, Camarero, Gutierrez, Bochini, & Galleti, 2001), and it was found that: white-rot fungi have the capability to degrade lignin as well as other wood cell-wall components, although the rate at which they do this also differs. Selective (or preferential) and simultaneous white-rots are categorized on the basis of removal of cell-wall constituents. Selective white-rots degrade hemicelluloses and lignin, resulting in defibrillation through dissolution of the middle lamella. In contrast, simultaneous or nonselective fungi remove lignin, hemicelluloses and cellulose at similar rates, resulting in homogeneous decay of the cell wall. Soft-rot fungi remove all cell-wall constituents, resulting in collapse of cell walls. Type-I soft-rot fungi cause decay that is erosive and attack all cell-wall layers simultaneously and removes all polymers at similar rates, while type-II selectively attack mostly polysaccharides in secondary wall layers, resulting in some developing typical cavities.

The wood-decaying fungi may display antagonistic interactions resulting in faster nutrition exploitation, or in parasitism, or may form deadlock interactions, where no hyphae of one species can enter the territory occupied by the other. Interactions may be synergistic, i.e. species can act in coordination to degrade the same substrate. A typical result of pathogenic and antagonistic interactions is oxidative stress creating reactive oxygen species (ROS), which in turn play a role in fungal wood decay.

FT-IR spectroscopy is a useful technique for studying wood decay chemistry, since minimal sample preparation is required and very small quantities of wood can be analyzed (a few milligrams) providing many and detailed structural information. FT-IR has previously been used to characterize the chemistry of wood (Faix, 1992; Pandey, 1999; Popescu et al., 2007) and determine lignin content in pulp, paper and wood (Rodrigues, Faix, & Pereira, 1998). It has also been used to analyze the chemical changes occurring during wood weathering, decay and chemical treatments (Moore & Owen, 2001) or natural ageing (Popescu, Vasile, Popescu, & Singurel, 2006).

* Corresponding author. Tel.: +40 232217454; fax: +40 232211299.
E-mail address: mihapop@icmpp.ro (C.-M. Popescu).

0144-8617/$ - see front matter © 2009 Elsevier Ltd. All rights reserved.
doi:10.1016/j.carbpol.2009.08.015

Fungal decay of wood has been studied using FT-IR by several researchers. Faix, Bremer, Schmidit, and Stevanovic (1993) used this technique to monitor changes in beech wood decayed by white-rot fungi. Korner, Faix, and Wienhaus (1992) investigated the effects of brown-rot decay (by *Fomitopsis pinicola* and *Coniophora puteana*) on the chemistry of Scots pine. Ferraz, Baeza, Rodrigues, and Freer (2000) used FT-IR-DRIFT spectroscopy to characterize changes in wood of *Pinus radiata* and *Eucalyptus globulus* decayed by white and brown-rot fungi. However, most published works describe qualitative changes in the FT-IR spectra following decay over long exposure periods. Information on relative changes in lignin/carbohydrate composition of wood decayed for short exposure periods and changes over time is limited.

In this paper, we present a detailed FT-IR spectroscopic analysis of the chemical changes occurring in a softwood (*Tillia Cordata* Mill.) decayed by the soft-rot *Trichoderma viride*. Samples were decayed to different levels (determined by weight loss) through exposing samples to fungi for different periods from 2 to 12 weeks.

2. Experimental

2.1. Materials

Lime wood sheets ($50 \times 30 \times 5$ mm) were oven-dried at 103 ± 2 °C, until constant weight was obtained and then weighed. Samples were sterilized and exposed to *T. viride* in Petri dishes containing 2% malt extract, 2% dextrose, 2% agar, in distilled water, pre-inoculated 1 week prior to the test and then they were incubated at 28 °C for 12 weeks.

From Fig. 1, it is easy to observe the way in which *T. viride* starts to colonize and develops on the wood surface. After 49 days of exposure the fungus reaches the maturity and start to sporulate, this being more easy observable after 77 days of exposure.

2.2. Characterization methods

Powdered wood sample prevailed mainly on surface was sieved and the fraction with average diameter less than 0.2 mm was retained for analysis.

FT-IR spectra were recorded on solid samples in KBr pellets by means of a FT-IR Bomem MB-104 spectrometer (Canada) with a resolution of 4 cm^{-1}. The concentration of the sample in the tablets was constant of 5 mg/500 mg KBr. Five recordings were performed for each sample after successive milling and the evaluations were made on the average spectrum obtained from these five recordings. Processing of the spectra was done by means of Grams/32 program (Galactic Industry Corporation).

2D FT-IR correlation intensities were calculated using an own MATLAB programme (Popescu, Ph.D. Thesis, 2009) using the generalized 2D-correlation method developed by Noda (1993). In 2D-correlation analysis, two kinds of correlation maps synchronous and asynchronous are generated from a set of dynamic spectra obtained from the modulation experiment (Noda, 1993). Synchronous 2D-correlation spectra represent the simultaneous or coincidental changes of spectral intensities measured at the wavenumbers v_1 and v_2. Correlation peaks appearing at the diagonal position ($v_1 = v_2$) correspond to the linear evolution of a given species along the induced perturbation. However, such a correlation peak does not provide major information since its intensity value only depends on change in single absorbance band intensity. Thus, such a correlation peak is considered as an auto-peak (Czarnecki, 1998). On the other hand, correlation peaks appearing out of the diagonal position ($v_1 \neq v_2$) correspond to the simultaneous changes of spectral signals at two different wavenumbers, which may be positively correlated (the two signals evolve correlatively in the same direction) or negatively correlated (the two signals evolve correlatively in opposite directions) with each other. The asynchronous 2D-correlation spectra represent sequential, or unsynchronized, changes of spectral intensities at the wavenumbers v_1 and v_2. The spectrum is antisymmetric with respect to the diagonal line and, thus, correlation peaks only appears out of the diagonal line. An asynchronous correlation peak develops only if the intensities of the two dynamic spectral intensities vary out of phase (delayed or accelerated) with each other. The sign of an asynchronous correlation peak may be positive if the intensity change at v_1 occurs predominantly before v_2, or it may be negative if the change occurs after v_2. According to Noda (1993), the sign of asynchronous peaks provides very useful information about the temporal sequence of events taking place during the studied process.

Combined synchronous spectra and asynchronous spectra generated during exposure time of the lime wood to the fungi, the variation sequence of different groups could be estimated. The rules are as follows: if the cross-peaks in synchronous spectrum (v_1, v_2) are positive (assume that $v_1 > v_2$), and the cross-peak at

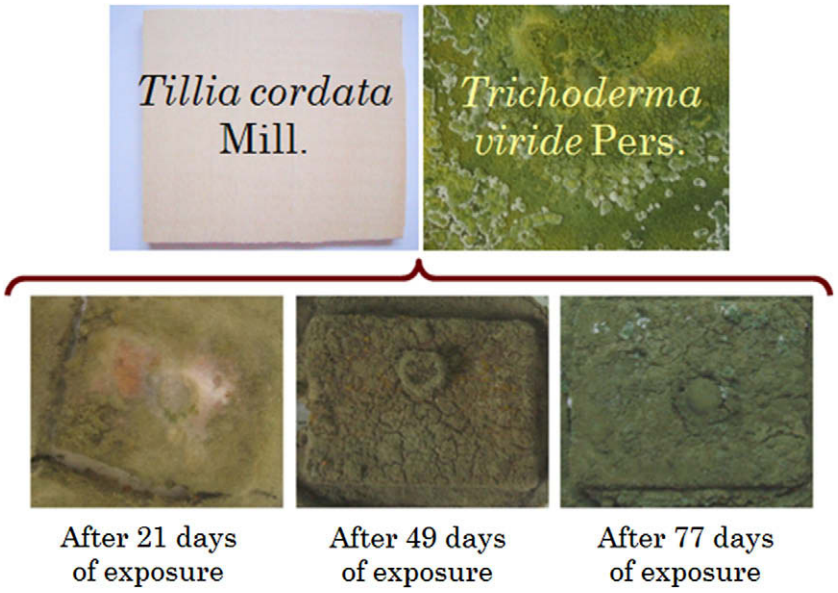

Fig. 1. Pictures with different stages of decay with *T. viride* on wood.

the same position in asynchronous spectrum is also positive, then the change at ν_1 may occur prior to that of ν_2. If the cross-peak in asynchronous spectrum is negative, then the change at ν_2 may occur prior to that of ν_1. If the ν_1, ν_2 in synchronous spectra are negative, the rules are reversed.

3. Results and discussion

3.1. Mass loss data

During a 12 weeks period, at each 1-week interval, two lime wood samples were prevailed from exposure medium, mycelium were removed from their surfaces by repeated washing with twice distilled water and then the samples were oven-dried up to constant weight. The mass losses of individual samples were calculated, and used to determine mean weight percentage losses.

Average mass losses for lime wood blocks at 84 days exposure to *T. viride* was 14.3 wt%. The fungus action manifested by continuous decrease of sample mass 0.05 wt%/day in the first 34–35 days and is five times faster (0.24 wt%/day) in the next period of 50 days. By visual observation it has been established that the growing period of fungus on the surface of wood sample was of about 35 days; then the fungus reached the maturity and forms the spores and its attack is much aggressive.

3.2. FT-IR spectroscopy

FT-IR spectra of undecayed and decayed lime wood are shown in Figs. 2 and 3. Because of their complexity the spectra were separated in two regions, namely: the OH stretching vibrations in 3800–2700 cm^{-1} region and "fingerprint" region in 1800–400 cm^{-1} region.

In 3800–2700 cm^{-1} region, strong hydrogen bonded (O—H) stretching absorptions and prominent C—H stretching absorptions were observed. The hydroxyl stretching region of the spectrum is particularly useful for elucidating hydrogen-bonding patterns because, in favorable cases, each distinct hydroxyl group gives a single stretching band at a frequency that decreases with increasing strength of hydrogen bonding.

According to the literature (Kondo, 2005; Nishiyama, Sugiyama, Chanzy, & Langan, 2003; Perez & Mazeau, 2005) there are inter- and intra-molecular H-bonds in cellulose I and in lignin; a secondary OH group at the C3 position forms a H-bond with an O5 atom of the adjacent ring (O3—H3···O5 intramolecular H-bond), and another secondary OH group at the C2 position forms a H-bond with an O6 atom of the adjacent ring (O2—H2···O6 intramolecular H-bond). A primary OH group at the C6 position is involved in an H-bond with an O3 atom in the neighboring chain (O6—H6···O3′ intermolecular H-bond). Also, aliphatic hydroxyl groups in lignin have the potential to form stronger intermolecular hydrogen bonds than phenolic hydroxyl groups. These H-bonds are considered to be responsible for various properties of native cellulose, lignin and of course wood itself. Thus, a mixture of inter- and intramolecular hydrogen bonds is considered to cause the broadening of the OH band in the IR spectra.

In Fig. 2, the IR spectra and the second derivative of these spectra in the 3800–2700 cm^{-1} region of the undecayed and decayed lime wood samples are shown.

Generally, the second derivative of IR spectra can obviously enhance the apparent resolution and amplify small differences of IR spectrum. These were obtained with the Savitsky–Golay method (second-order polynomial with 15 data points) using Grams 32 program.

From the Fig. 2a it can be observed that all bands in this region have lower intensities in the spectra of decayed wood samples,

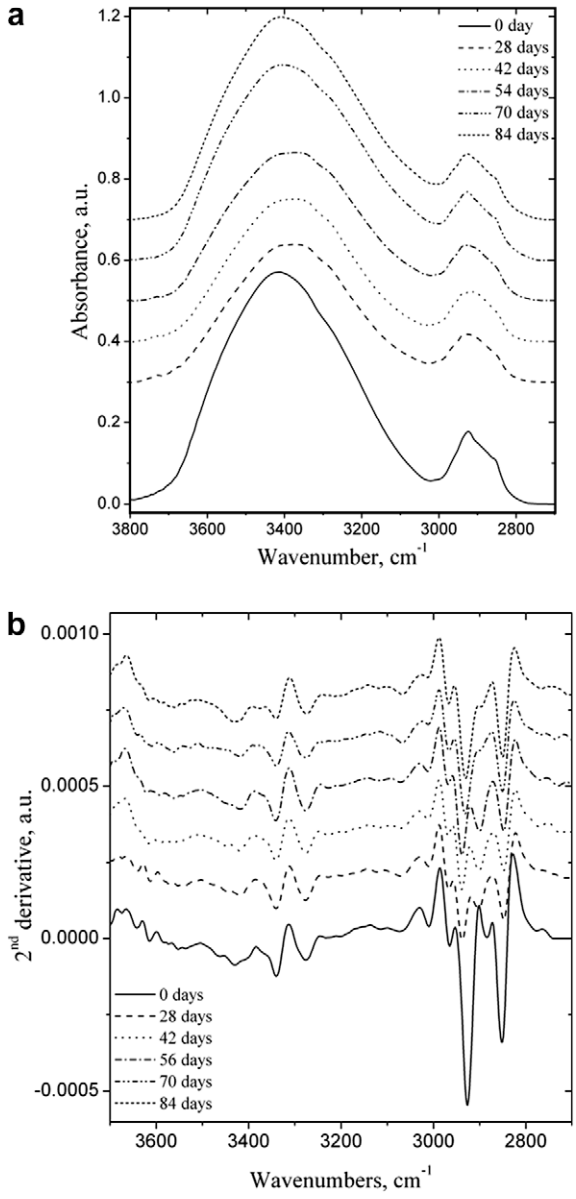

Fig. 2. FT-IR spectra (a) and the second derivative spectra (b) of biodegraded lime wood samples in 3800–2700 cm^{-1} region.

than in the undecayed one. From second derivative (Fig. 2b) it was possible to identify all bands which are present in this region which are summarized in Table 1.

The most significant absorbance bands in the 3800–2700 cm^{-1} region have been assigned to valence vibrations of OH groups which form inter- and intra-molecular H-bonds and to valence vibrations of C—H in wood samples, based on previous literature data (Pandey & Theagarajan, 1997; Popescu et al., 2007; Schwanninger, Rodrigues, Pereira, & Hinterstoisser, 2004).

Bands observed in the 3800–2700 cm^{-1} region (Fig. 2a) are assigned to the stretching modes of OH groups of wood. A broad band with a maximum around 3415 cm^{-1} was observed in the spectrum of the undecayed lime wood sample, while in the spectra of decayed wood, this maximum is shifted to lower wavenumbers. The intensity of this band decreases in the spectra of the decayed wood. These observations reflect variations in the hydrogen-bond structure of wood when biodegradation process proceeds.

According to the literature data an intramolecular hydrogen bond in a phenolic group (in lignin) was observed at around 3560–3550 cm^{-1}, also multiple formation of an intermolecular

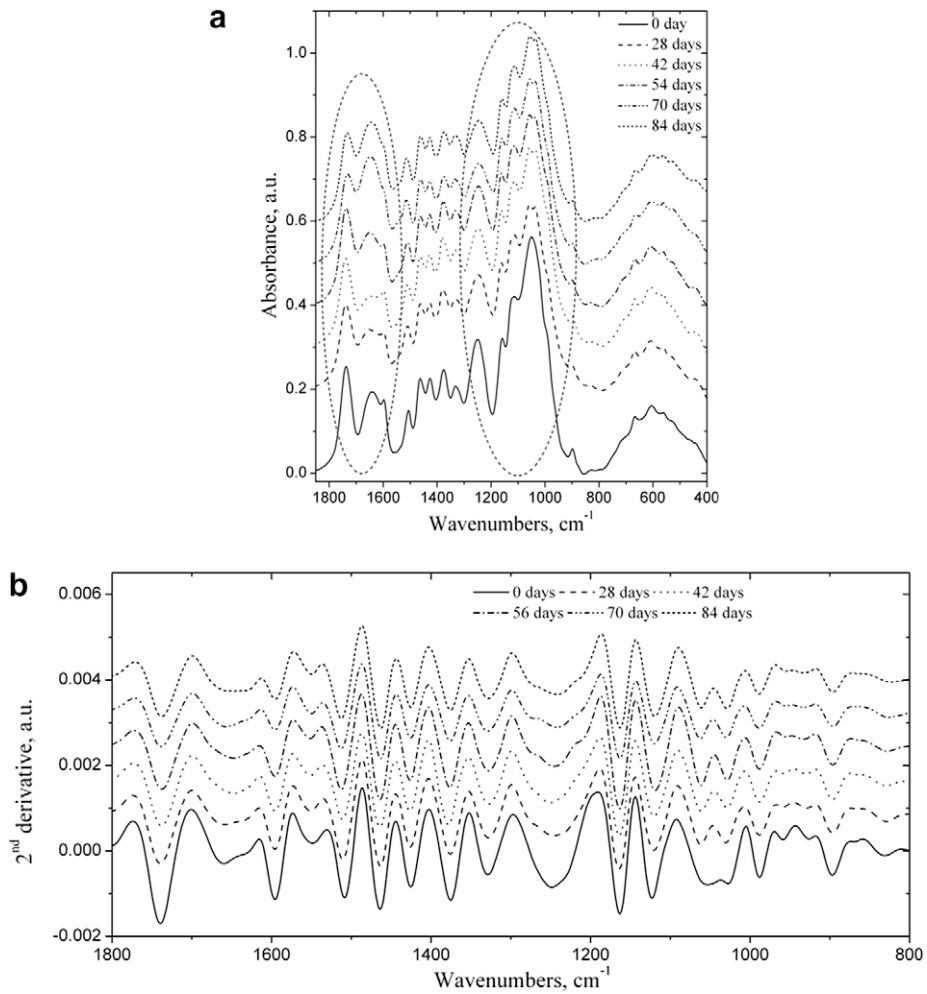

Fig. 3. FT-IR spectra (a) and the second derivative spectra (b) of biodegraded lime wood samples in 1800–400 cm^{-1} region.

Table 1
The characteristic bands in FT-IR spectra of the studied lime wood samples in 3800–2700 cm^{-1} region.

Band assignment	Wavenumber (cm^{-1})	Decayed
Absorbed water weakly bound and intramolecular hydrogen bond in a phenolic group (in lignin)	3563	+
Multiple formation of an intermolecular hydrogen bond between phenolic groups and their combinations with alcoholic groups	3452	–
O(2)H···O(6) intramolecular stretching modes (in cellulose)	3427	+
O(3)H···O(5) intramolecular in cellulose	3340	–
O(6)H···O(3) intermolecular in cellulose Iβ (3270)	3274	–
O(6)H···O(3) intermolecular in cellulose Iα (3240)	3213	+
Multiple formation of an intermolecular hydrogen bond between biphenol and other phenolic groups (in lignin)	3114	+
C—H stretching in methyl and methylene groups	2965	+
Asymmetric methoxyl C—H stretching	2929	–
	2900	+
Symmetric CH_2 stretching	2894	–
	2847	–

hydrogen bond between phenolic groups and their combinations with alcoholic groups may form a band at around 3452 cm^{-1} (Kubo & Kadla, 2005).

In the same time, in cellulose an intramolecular hydrogen bond vibration, derived from O2—H2···O6, could be expected at 3420 cm^{-1}. The intermolecular hydrogen bonds involving the C6 position (primary hydroxyl groups) result in the formation of crystalline regions and contribute to the O—H band at 3420 cm^{-1}. These bands show variation of the maxima with few wavenumbers to lower values in the spectra of decayed wood. The frequencies for the O5—H5···O3 intramolecular hydrogen bond can be found between 3350 and 3375 cm^{-1} according to the literature (Watanabe, Morita, & Ozaki, 2006; Watanabe, Morita, & Ozaki, 2007; Šturcová, His, Apperley, Sugiyama, & Jarvis, 2004), in the spectra of the lime wood being observed at 3340 cm^{-1}. A shift to lower frequencies can probably be explained to be a result of the stretching of the cellulose molecules parallel to the main fiber direction. A decreasing intensity of the O3—H3···O5 intramolecular hydrogen vibration clearly indicates its importance in the loading of the cellulose chain, comparable to that of the C—O—C bridge.

In this region, also characteristic bands are assigned to the two crystalline allomorphs, cellulose Iβ and cellulose Iα. A peak at

3213 cm^{-1} was assigned to hydrogen bonds formed only in cellulose Iα phase by Sugiyama, Persson, and Chanzy (1991). This peak is not observed in an IR spectrum of cellulose Iβ (Sugiyama et al., 1991; Watanabe et al., 2006). Especially, the band at 3213 cm^{-1} is attributed to the O6—H6···O3 intramolecular hydrogen bonds existing only in triclinic Iα cellulose (Sugiyama et al., 1991), whereas that near 3274 cm^{-1} seems to be proportional to the amount of monoclinic phase Iβ; therefore, it can be assigned to this phase. The band at 3274 cm^{-1} is shifted to higher wavenumbers with maximum 4 cm^{-1}, while the band at 3213 cm^{-1} is shifted to lower wavenumbers with maximum 10 cm^{-1}, and in the same time the intensities of these bands are decreasing with exposure time to the fungus.

This means that structure of cellulose starts to present some modifications with increasing exposure time to biodegradation with *T. viride*. Also, the intensity of the band from 3452 cm^{-1} which in the derivative spectrum of the lime wood undegraded is not observed; start to increase from the spectrum of lime wood degraded 35 days. This band is assigned to multiple formation of an intermolecular hydrogen bond between phenolic groups and their combinations with alcoholic groups from lignin, meaning that after 35 days of exposure to decay part of cellulose and hemicelluloses are removed, being observable stretching vibrations of different groups from lignin and many contacts between components are possible.

The O—H stretching region was deconvoluted into Gaussian components. This procedure allows band positions to be compared between spectra when the band widths and the extent of overlapping differ. After deconvolutions seven O—H stretching bands were identified and used to calculate energy and hydrogen bonding distance.

The energy of the hydrogen bonds (Table 2) has been evaluated using the following formulae (Struszczyk, 1986):

$$E_H = \frac{1}{k}\left[\frac{v_o - v}{v_o}\right] \quad (1)$$

where v_o is standard frequency corresponding to free —OH groups (3650 cm^{-1}) and v is the frequency of the bonded —OH (3565, 3465, 3439, 3350, 3269 and 3222 cm^{-1}) groups, while k is a constant ($1/k$ is equal with $2.625 * 10^2$ kJ).

The calculated energies (Table 2) are almost constant for band from 3340 cm^{-1} (O(3)H···O(5) intramolecular in cellulose), while for band from 3213 cm^{-1} (O(6)H···O(3) intermolecular in cellulose Iα) are increasing with exposure time to the fungus. On the other hand, for the bands from 3563 cm^{-1} (absorbed water weakly bound and intramolecular hydrogen bond in a phenolic group (in lignin)), and 3445 cm^{-1} (multiple formation of an intermolecular hydrogen bond between phenolic groups and their combinations with alcoholic groups), 3427 cm^{-1} (O(2)H···O(6) intramolecular stretching modes (in cellulose)), 3274 cm^{-1} (O(6)H···O(3) intermolecular in cellulose Iβ) the calculated energies are decreasing over experiment and the energies for the band at 3114 cm^{-1} (multiple formation of an intermolecular hydrogen bond between biphenol and other phenolic groups (in lignin)) are decreasing from undecayed wood to wood exposed up to 28 days to microorganisms attack, and then start to increase up to 84 days. Decreasing of the energy of the hydrogen bonding is due to a shifting of the corresponding vibration bands to a higher wavenumbers.

The hydrogen bonding distances were evaluated, being of 2.83, 2.80, 2.78, 2.76, 2.75, 2.73 Å for each band, and are the same in all wood samples for all types of H-bonds. The differences in band position did not influence the hydrogen bonding distance.

In addition, there are many well-defined peaks in the "fingerprint" region between 1850 and 400 cm^{-1}. The peaks maxima from the wood spectra are shown in Table 3 (Pandey & Theagarajan, 1997; Popescu et al., 2007; Schwanninger et al., 2004).

FT-IR spectra of lime wood exposed to *T. viride* for 84 days show changes at very early stages of decay. The intensities of carbohydrate bands decrease with exposure time to the fungus. In contrast, intensities of absorption bands resulting totally or partially from lignin increase as decay progresses. After 35 days exposure the band from 1596 cm^{-1} is overlapped with band at 1645 cm^{-1}, being observable only from derivative spectra (Fig. 3b).

The band at 1245 cm^{-1} decreases in intensity and become wider with increasing exposure time to the fungus. It has been shown that the syringyl type (the major type of hardwood lignin) absorbs only at 1230 cm^{-1}. Although hardwood lignin also contains guaiacyl moieties, the absorption band at 1268 cm^{-1} may have been suppressed by a strong absorption at 1245 cm^{-1}. From derivative spectra can be observed after 49 days of exposure a very small shoulder which increase in intensity at 1268 cm^{-1}. The appearance of the 1268 cm^{-1} band in decayed lime wood can be mainly due to decrease in the intensity of 1245 cm^{-1} band resulting from xylan degradation, since this band results partially from the C—O in xylan.

The band at 1738 cm^{-1} assigned to unconjugated C=O in xylans (hemicellulose) is decreasing with exposure time to the fungus, the presence of this band in wood decayed for 84 days is due to residual xylan.

Also the decrease in the intensity of the 1650 cm^{-1} band after 28 days exposure results from an increase of carbonyl moieties as decay progresses.

We have calculated the ratios of the heights of lignin peaks at 1511 against peaks at 1462 and 1425 cm^{-1} (due to C—H, deformation of methyl and methylene). There is only a small decrease in the ratio after decay. Values for ratios I_{1462}/I_{1511} and I_{1425}/I_{1511}, decreases after decay of 84 days, from 1.24 to 1.06 and from 0.74 to 0.62, respectively. This small decrease may be due to xylan decay, since both of peaks have a contribution from carbohydrates.

In the same time was possible to estimate by FT-IR spectra, the crystallinity degree of undecayed and decayed wood samples, using an expeditious method proposed by Hulleman, Van Hazendonk, and Van Dam (1994) for cellulose I, which is based on the observation that the band at 1280 cm^{-1}, assigned to the C—H bending mode, increases with increasing crystallinity, whereas the band assigned to the C—O—C stretching mode of the pyranose ring, at 1200 cm^{-1}, is sensitive to that parameter. The ratio between the absorption intensities of these two bands ($R_{c,h} = I_{1280}$/

Table 2
The energy of the hydrogen bonding for studied samples.

Samples	Hydrogen bonding energy (E_H)						
	3563 cm^{-1}	3445 cm^{-1}	3427 cm^{-1}	3340 cm^{-1}	3274 cm^{-1}	3213 cm^{-1}	3114 cm^{-1}
Lime wood – 0 days	6.89	14.74	16.74	22.29	27.14	31.43	38.55
Lime wood – 28 days	6.90	14.60	16.54	22.25	27.11	31.28	38.04
Lime wood – 42 days	6.76	14.31	16.68	22.29	26.97	31.86	38.11
Lime wood – 56 days	6.54	14.24	16.68	22.22	26.97	32.07	38.26
Lime wood – 70 days	6.54	14.17	16.68	22.29	26.97	32.22	38.26
Lime wood – 84 days	6.40	14.09	15.89	22.37	29.90	32.22	38.47

Table 3
The characteristic bands in FT-IR spectra of the studied lime wood samples 1800–400 cm^{-1} region.

Band assignment	Wavenumber (cm^{-1})	Decayed
Unconjugated C=O in xylans (hemicellulose)	1737	–
Absorbed O—H and conjugated C—O	1645	–
Xyloglucan C=O vibration of the carboxylic acids	1596	–
C=C of aromatic skeletal (lignin)	1512	=
C—H deformation in lignin and carbohydrates	1462	–
C—H deformation in lignin and carbohydrates	1424	–
C—H deformation in cellulose and hemicellulose	1375	–
C—H vibration in cellulose and C_I—O vibration in syringyl derivatives	1330	–
Guaiacyl ring breathing, C—O stretch in lignin and for C—O linkage in guaiacyl aromatic methoxyl groups	1268	+
Syringyl ring and C—O stretch in lignin and xylan	1245	–
C—O—C vibration in cellulose and hemicellulose	1164	–
Aromatic skeletal and C—O stretch	1120	–
C—O stretching mainly from C(3)—O(3)H in cellulose I	1062	–
C—O and C—C stretching ring in cellulose and hemicelluloses	1041	–
Aromatic C—H in plane deformation	1028	+
C—O valence vibration	988	–
	954	–
Pyran ring stretching	933	–
C—H deformation in cellulose	897	–

I_{1200}) was used to determine crystallinity of lime wood samples (Ilharco, Garcia, Lopes da Silva, & Ferreira, 1997).

$$x_c = 1.06 * R_{c,h} + 0.19 \quad (2)$$

This correlation is valid only in the range $0.26 \leqslant x_c \leqslant 0.75$, the cellulose crystallinity limits used by Hulleman et al. (1994). The values obtained are listed in Table 4.

These values obtained for crystallinity degree from FT-IR bands ratios are decreasing with exposure time to the fungus, therefore the structure becomes less ordered.

It is important to mention that most of the bands in the "fingerprint" region have contributions from all the wood constituents and a careful interpretation of IR data is needed. For this reason an additional method was used to give much insight in spectral features.

The *2D-correlation IR spectroscopy* can enhance the spectral resolution; it can obtain new information, which cannot be acquired by using conventional IR and its derivative spectra can be obtained. There is a unique advantage of 2D-correlation IR spectra to identify and distinguish complex systems.

2D-correlation spectra generated from the exposure time-dependent infrared spectra of the studied decayed wood were obtained. Correlation spectra clearly show the presence of synchronous and asynchronous correlation peaks among different modes of molecular vibrations. In practice, when 2D-correlation analyses are done, it is usually more convenient to scan only a part of the correlation map to pick up a useful local feature of the correlation intensity profile rather than displaying the entire spectral region. Therefore, the contour maps in the 3900–2750, 1900–1560, and 1560–860 cm^{-1} regions for two time ranges of 0–35 days and 35–84 days (see mass loss data) were evaluated.

In the synchronous 2D-correlation spectrum of the exposure time range of 0–35 days (Fig. 4a), one auto-peak at $\Phi(3430, 3430) > 0$ and a pair of cross-peaks of $\Phi(3430, 2922) > 0$ are observed, implying that both bands around 3430 and 2922 cm^{-1} decrease with the increase in the exposure time. Similar tendencies are observed for the synchronous 2D-correlation spectra of the other exposure time region (Fig. 4c), only the peak positions are shifted to 3419 and 2927 cm^{-1}. The shifts to a lower wavenumber of the auto-peak around 3430 cm^{-1} with the progress of the biodegradation process indicate that the O(2)H···O(6) intramolecular hydrogen bonds become stronger. The auto-peak at 3430/3419 cm^{-1} is very broad. Thus, it seems that this auto-peak consists of more than one peak, these bands decrease in same direction with increasing exposure time to the fungus.

One auto-peak and a shoulder peak are observed in the autocorrelation spectra of the both exposure time ranges (Fig. 4b and d). The positions of the auto-peaks at 3430 and 3281 cm^{-1} for the 0–35 days range, and 3419 and 3263 cm^{-1} for the 35–84 days range correspond to the positions of the peaks identified in the second derivative spectra (Fig. 2b). The bands at 3281 and 3263 cm^{-1} are attributed to O(6)H···O(3) intermolecular in cellulose Iβ. These results indicate that the disruption of the inter- and intrachain H-bonds in cellulose takes place.

Fig. 5 shows the asynchronous 2D-correlation spectra constructed from the exposure time-dependent IR spectral variations in the time ranges of 0–35 (a) and 35–84 (b) days. The negative correlation areas in the 2D-correlation spectra are given in gray color. In the asynchronous spectrum (Fig. 5a) six bands at 3572, 3432, 3332, 3215, 2922 and 2848 cm^{-1} are identified. These bands are assigned to different O—H and C—H vibrations. Positive peaks at $\Psi(3572, 3332) > 0$ and $\Psi(3572, 2922) > 0$ and negative peak at $\Psi(3332, 3215) < 0$ were identified. Based on the fundamental rule of an asynchronous spectrum (Noda, 1993), the spectral intensity change at 3572 cm^{-1} occurs before those at 3332, 3215 and 2922 cm^{-1} in the exposure time range of 0–35 days.

Thus, applying the Noda's rules was obtained the following sequence of the spectral intensity changes: 3572 > 3215 > 3432 > 3332 > 2922, 2848 cm^{-1} in the exposure time to the fungi range of 0–35 days. This sequence means that the moment of free OH groups is changing first, followed by the O(6)H···O(3) intermolecular, O(2)H···O(6) intramolecular, O(3)H···O(5) intramolecular

Table 4
Crystallinity degree evaluated by FT-IR spectroscopy.

Samples	Lime wood – 0 days	Lime wood – 35 days	Lime wood – 49 days	Lime wood – 70 days	Lime wood – 84 days
Cr. I.	50.8	47.4	46.0	44.3	43.8

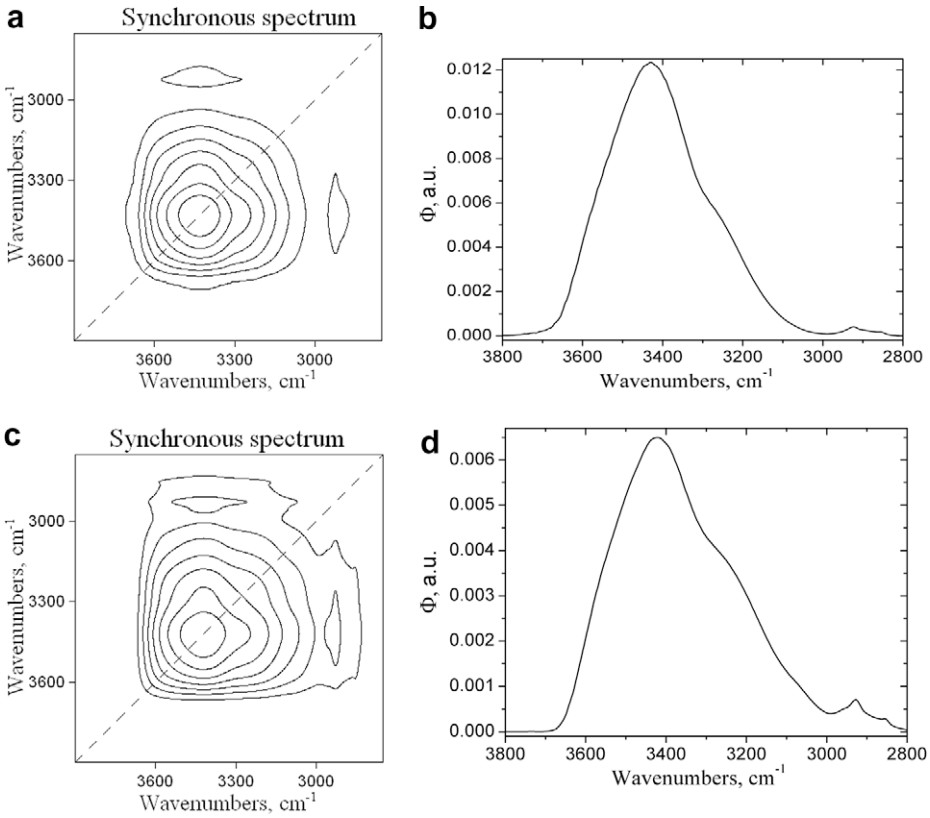

Fig. 4. Synchronous 2D-correlation spectra (a and c) and autocorrelation spectra (b and d) in the 3800–2800 cm^{-1} region constructed from the exposure time-dependent IR spectra. Biodegradation time ranges of 0–35 (a and b) and 35–84 (c and d) days.

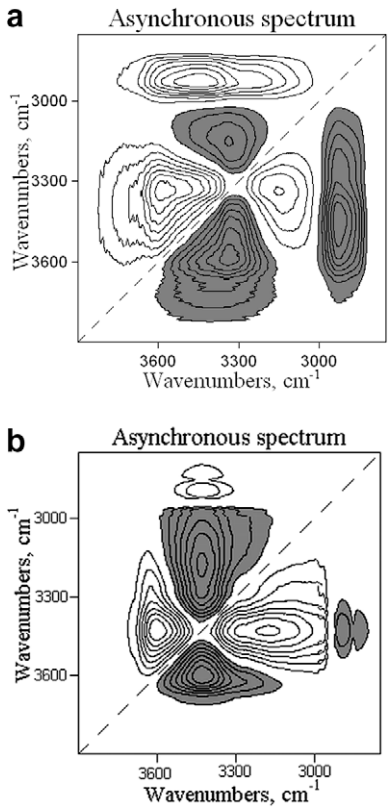

Fig. 5. Asynchronous 2D-correlation spectra in the 3800–2800 cm^{-1} region constructed from the exposure time-dependent IR spectra. Biodegradation time ranges of 0–35 (a) and 35–84 (b) days.

vibrations in cellulose, and symmetric and asymmetric C—H vibrations. The decreasing of the intensity of these bands and also the above sequence, evidence the order in which the cellulose aggregate linkages are broken due to biodegradation.

In Fig. 5b, the asynchronous 2D-correlation spectrum in the 3800–2800 cm^{-1} region constructed from the exposure time-dependent IR spectra in the 35–84 days exposure time range is shown. In this case were observed six bands at 3560, 3419, 3341, 3276, 2927 and 2849 cm^{-1}. In this case the sequence of the spectral intensity changes is as follows: 3560 > 3276 > 3419 > 3341 > 2927, 2849 cm^{-1}, the order being the same as in the case of 0–35 days range time.

The second region, 1900–1560 cm^{-1} the 2D-correlation spectra are similar for both exposure times ranges 0–35 and 35–84 days, thus the explanations will be made only for first range.

Thus in synchronous correlation spectrum (Fig. 6a), two auto-peaks at $\Phi(1732, 1732) > 0$ and $\Phi(1640, 1640) > 0$ and a pair of cross-peaks of $\Phi(1732, 1640) > 0$ are observed, implying that both bands around 1732 and 1640 cm^{-1} decrease with the increase in the exposure time.

Two auto-peaks and a very small shoulder are observed in the autocorrelation spectrum in the 1900–1560 cm^{-1} region constructed from the exposure time-dependent IR spectra (Fig. 6b). The positions of the auto-peaks at 1732, 1640 and 1597 cm^{-1} almost completely correspond to the positions of the peaks identified in the second derivative spectra (Fig. 3b). These bands are attributed to unconjugated C=O in xylans (hemicellulose), absorbed O—H and conjugated C—O and xyloglucan C=O vibration of the carboxylic acids, respectively.

The asynchronous 2D-correlation spectrum constructed from the exposure time-dependent IR spectral variations in the time range of 0–35 days (Fig. 7) show three bands at 1730, 1640 and

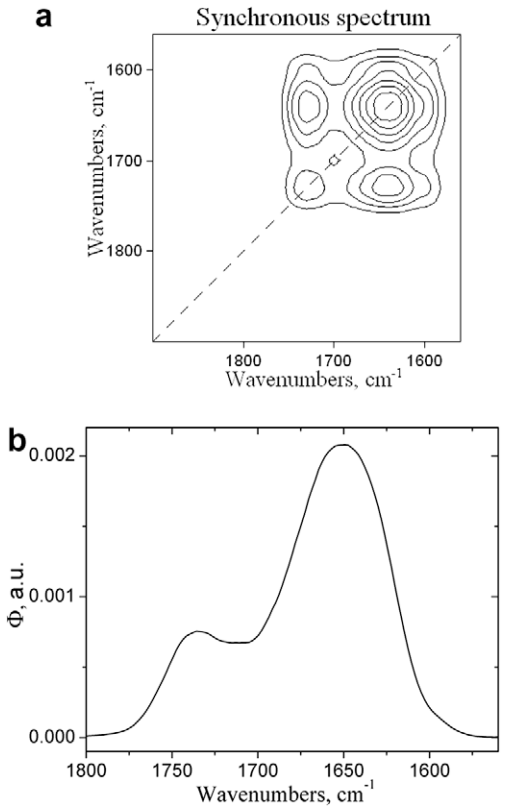

Fig. 6. Synchronous 2D-correlation spectrum (a) and autocorrelation spectrum (b) in the 1900–1560 cm^{-1} region constructed from the exposure time-dependent IR spectra. Biodegradation time range of 0–35 days.

1597 cm^{-1}. Positive peak at $\Psi(1640, 1597) > 0$ and negative peak at $\Psi(1730, 1640) < 0$ were identified. Based on the fundamental rule of an asynchronous spectrum, the spectral intensity change at 1640 cm^{-1} occurs before those at 1730 and 1597 cm^{-1}.

Thus the following sequence of the spectral intensity changes: 1640 > 1730 > 1597 cm^{-1} was obtained. This sequence means that the moment of conjugated C—O is changing first, followed by the unconjugated C=O in xylans (hemicellulose), and then xyloglucan C=O vibration of the carboxylic acids.

The fungi use extracellular reactive oxygen species (ROS) to degrade lignocelluloses materials (Hammel, Kapich, Jensen, & Ryan, 2000). **.**OH abstracts hydrogen atoms from the sugar subunits of polysaccharides such as cellulose with high rate constants. These reactions produce transient carbon-centered radicals that react rapidly with O_2 to give ROO**.** species. If the peroxyl radical already carries a hydroxyl group on the same carbon, it eliminates **.**OOH. If it carries no α-hydroxyl group, it undergoes a variety of oxidoreductions, some of which result in cleavage of the polysaccharide chain. The modification of these bands with increasing the exposure time to the fungi is due to this process, resulting complex product mixtures.

In the 1560–1195 cm^{-1} region, the 2D-correlation spectra are also similar for both exposure times ranges 0–35 and 35–84 days, thus the explanations will be made only for first range.

Fig. 8a show the synchronous 2D-correlation spectrum in the 1560–1195 cm^{-1} region constructed from the exposure time-dependent IR spectra. Here 5 auto-peaks at $\Phi(1458, 1458) > 0$, $\Phi(1425, 1425) > 0$, $\Phi(1377, 1377) > 0$, $\Phi(1328, 1328) > 0$ and $\Phi(1254, 1254) > 0$ and 10 pairs of cross-peaks of $\Phi(1458, 1425) > 0$, $\Phi(1458, 1377) > 0$, $\Phi(1458, 1328) > 0$, $\Phi(1458, 1254) > 0$, $\Phi(1425, 1377) > 0$, $\Phi(1425, 1328) > 0$, $\Phi(1425, 1254) > 0$, $\Phi(1377, 1328) > 0$, $\Phi(1377, 1254) > 0$, and $\Phi(1328, 1254) > 0$ are observed, implying that all bands around 1458, 1425, 1377, 1328 and 1254 cm^{-1} decrease with the increase in the exposure time to the fungi.

From the autocorrelation spectrum in the 1560–1195 cm^{-1} region constructed from the exposure time-dependent IR spectra (Fig. 8b), five auto-peaks were observed. The positions of the auto-peaks at 1460, 1426, 1377, 1330 and 1254 cm^{-1} correspond to those of the peaks identified in the second derivative spectra (Fig. 5b). These bands are attributed to C—H deformation in lignin and carbohydrates, C—H deformation in cellulose and hemicellulose, C—H vibration in cellulose and C_I—O vibration in syringyl derivatives, and syringyl ring and C—O stretch in lignin and xylan, respectively. It is known that *T. viride* is removing only carbohydrates, so the modification of these bands is contribution only to hemicelluloses and cellulose removal with exposure time to the fungi.

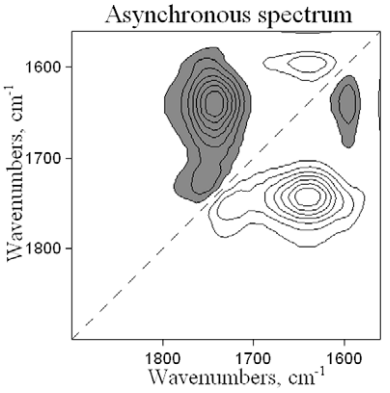

Fig. 7. Asynchronous 2D-correlation spectrum in the 1900–1560 cm^{-1} region constructed from the exposure time-dependent IR spectra. Biodegradation time ranges of 0–35 days.

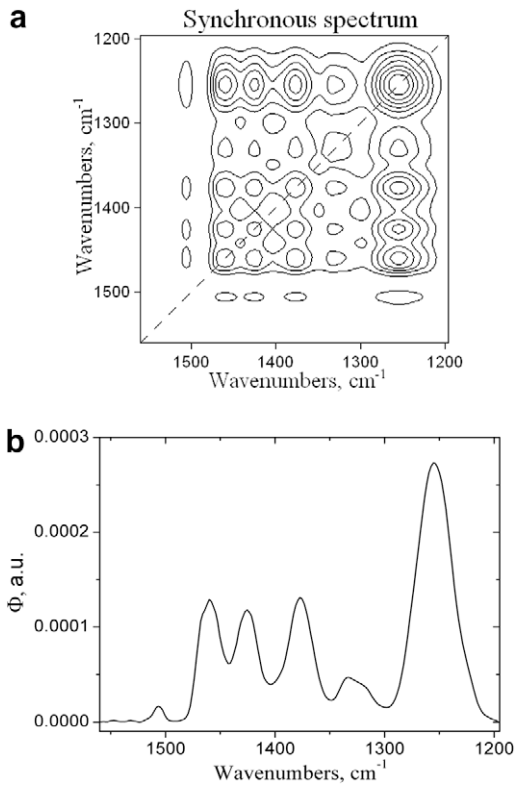

Fig. 8. Synchronous 2D-correlation spectrum (a) and autocorrelation spectrum (b) in the 1560–1195 cm^{-1} region constructed from the exposure time-dependent IR spectra. Biodegradation time range of 0–35 days.

The asynchronous 2D-correlation spectrum constructed from the exposure time-dependent IR spectral variations in the time range of 0–35 days (Fig. 9) show five bands at 1458, 1425, 1375, 1328 and 1254 cm^{-1}. Positive peaks at $\Psi(1425, 1248) > 0$, $\Psi(1375, 1254) > 0$ and $\Psi(1328, 1254) > 0$ and negative peaks at $\Psi(1458, 1425) < 0$, $\Psi(1458, 1375) < 0$, $\Psi(1458, 1328) < 0$, $\Psi(1458, 1254) < 0$, $\Psi(1425, 1375) < 0$, $\Psi(1425, 1328) < 0$, and $\Psi(1375, 1328) < 0$ were identified. The spectral intensity change at 1640 cm^{-1} occurs before those at 1730 and 1597 cm^{-1}.

Thus, the following sequence of the spectral intensity changes: 1375 > 1328 > 1425, 1458 > 1254 cm^{-1} was obtained. This sequence means that the moment of C—H deformation in cellulose and hemicelluloses is changing first, followed by the C—H vibration in cellulose, C—H deformation in carbohydrates, and then C—O stretch in xylan.

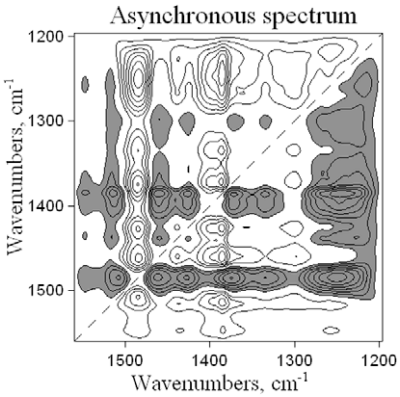

Fig. 9. Asynchronous 2D-correlation spectrum in the 1560–1195 cm^{-1} region constructed from the exposure time-dependent IR spectra. Biodegradation time ranges of 0–35 days.

The spectral region 1195–860 cm^{-1}, show different characteristics of the 2D-correlation IR spectra for exposure times ranges 0–35 and 35–84 days.

In the synchronous 2D-correlation IR spectrum of the exposure time range of 0–35 days (Fig. 10a), one broad auto-peak at $\Phi(1045, 1045) > 0$ is observed. Similar tendencies are observed for the synchronous 2D-correlation spectrum of the other exposure time region (Fig. 10c), only the peak position is shifted to 1037 cm^{-1}. This band is assigned to C—O and C—C stretching ring in cellulose and hemicelluloses. The shifts to a lower wavenumber of the auto-peak around 1045 cm^{-1} with the progress of the biodegradation process indicate a removal of cellulose and hemicelluloses structures. This auto-peak being very broad, it seems that it consists of more than one peak, these bands decrease in same direction with increasing exposure time to the fungi.

Three auto-peaks and two shoulder peaks are observed in the autocorrelation spectra of the both exposure time ranges. The positions of the auto-peaks at 1157, 1117, 1047, 1027 and 997 cm^{-1} for the 0–35 days range (Fig. 10b) and 1157, 1110, 1051, 1037 and 992 cm^{-1} for the 35–84 days range (Fig. 10d) correspond to the positions of the peaks identified in the second derivative spectra (Fig. 3b). The bands are attributed to C—O—C and C—O vibrations in cellulose and hemicelluloses. These results indicate an enzymatic oxidation and hydrolysis reactions on hemicelluloses and cellulose resulting oligomers and oxidized structures.

The asynchronous 2D-correlation spectra in the 1195–860 cm^{-1} region constructed from the exposure time-dependent IR spectra show different characteristics for both ranges. The asynchronous 2D correlation spectrum constructed from the exposure time-dependent IR spectral variations in the time range of 0–35 days (Fig. 11a) show five bands at 1163, 1114, 1051, 1034 and

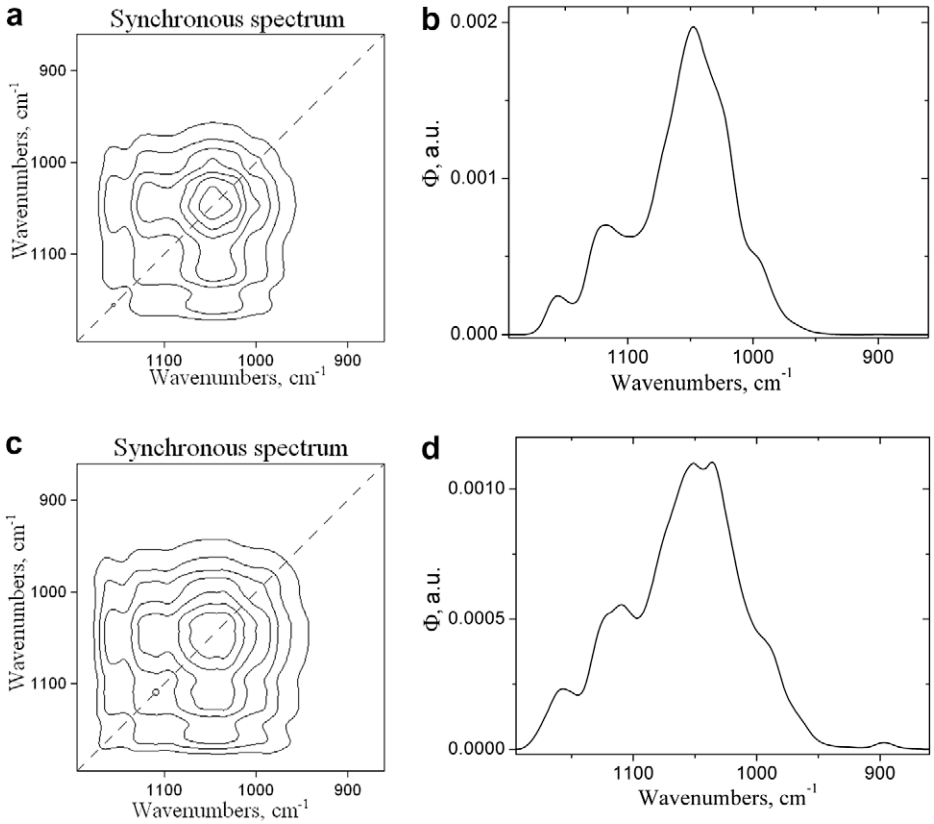

Fig. 10. Synchronous 2D-correlation spectra (a and c) and autocorrelation spectra (b and d) in the 1195–860 cm^{-1} region constructed from the exposure time-dependent IR spectra. Biodegradation time ranges of 0–35 (a and b) and 35–84 (c and d) days.

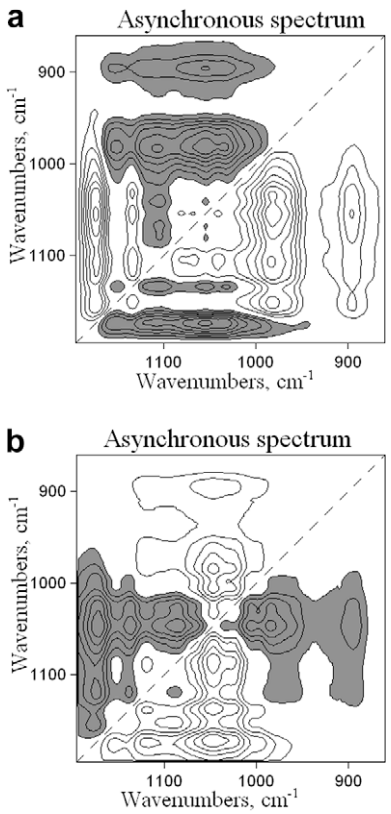

Fig. 11. Asynchronous 2D-correlation spectra in the 1195–860 cm^{-1} region constructed from the exposure time-dependent IR spectra. Biodegradation time ranges of 0–35 (a) and 35–84 (b) days.

995 cm^{-1}. Positive peaks at $\Psi(1114, 995) > 0$, $\Psi(1051, 995) > 0$, and $\Psi(1034, 995) > 0$ and negative peaks at $\Psi(1163, 1114) < 0$, $\Psi(1163, 1051) < 0$, $\Psi(1163, 1034) < 0$, $\Psi(1163, 995) < 0$, $\Psi(1114, 1051) < 0$, $\Psi(1114, 1034) < 0$, and $\Psi(1051, 1034) < 0$ were identified.

Based on the fundamental rule of a synchronous and an asynchronous spectrum was obtained the following sequence of the spectral intensity changes: 1034 > 1051 > 1114 > 995 > 1163 cm^{-1} in the exposure time to the fungi range of 0–35 days. This sequence means that the moment of C—O and C—C stretching ring in cellulose and hemicelluloses is changing first, followed by the C—O stretching mainly from C(3)—O(3)H in cellulose I, C—O vibration, C—O—C vibration in cellulose and hemicelluloses. For the second exposure time range, the following sequence was obtained: 992 > 1110 > 1037 > 1051 > 1157 cm^{-1}. Thus the moment of C—O vibration is changing first, followed by C—O and C—C stretching ring in cellulose and hemicelluloses and C—O stretching mainly from C(3)—O(3)H in cellulose I.

The results show that at the beginning of biodegradation process the formation of oxidized structures takes place; which occurs by the variation of C—O and C—C stretching ring in cellulose and hemicelluloses and increasing of the intensity of bands assigned to C—O vibrations. After 35 days of exposure to the fungi, the oxidation products are formed with a higher rate due to weakened structure of wood.

It is known that *T. viride* is a producer of cellulolytic and hemicellulolytic enzymes, especially enzymes hydrolyzing crystalline cellulose. In this fungus, cellulolytic enzyme system forms a synergistic complex of endoglucanases (endo-1,4-β-glucanases), which have been suggested to hydrolyze internal bonds and open free chain ends for cellobiohydrolases (exo-1,4-β-glucanases) to cleave off cellobiose units (reducing and non-reducing ends), which are broken down to glucose by β-glucosidase (Pérez, Muñoz-Dorado, de la Rubia, & Martínez, 2002). The endo-β-glucanases and cellobiohydrolases synergistically hydrolyze cellulose into small cellooligosaccharides, mainly cellobiose; whereas β-glucosidase hydrolyzes aryl- and alkyl-glucosides, cellobiose and cellodextrins.

The hemicelluloses xylan backbone is degraded by the ectoenzyme endo-1,4-β-xylanase within the xylose chain (endohydrolysis) to xylo-oligomers, xylobiose and xylose. Intracellular and/or membranebound xylan 1,4-β-xylosidase removes successively D-xylose residues from the non-reducing termini of small oligosaccharides. The side-groups are split by accessory enzymes: acetylesterase removes the acetyl groups, xylan α-1,2-glucuronidase hydrolyzes the α-D-1,2-(4-*O*-methyl)glucuronosyl links, arabinose side-groups in arabinoxylans are removed by α-arabinosidase (Schmidt & Czeschlik, 2006).

The molecules are first degraded by extracellular enzymes (ectoenzymes) into smaller fragments, which are taken up and then metabolized by intracellular enzymes to energy and fungal biomass. Independent of this place of action, an exoenzyme attacks at the end of a macromolecular substrate, while an endoenzyme splits within the molecule. Finally small molecules or fragments containing carboxyl, hydroxyl or carbonyl groups are formed, which are lost or remain in wood structures (Fig. 12).

4. Conclusions

FT-IR spectroscopy was used to examine qualitative and quantitative changes in carbohydrate components in wood decayed by soft-rots. In the present study has demonstrated that exposure

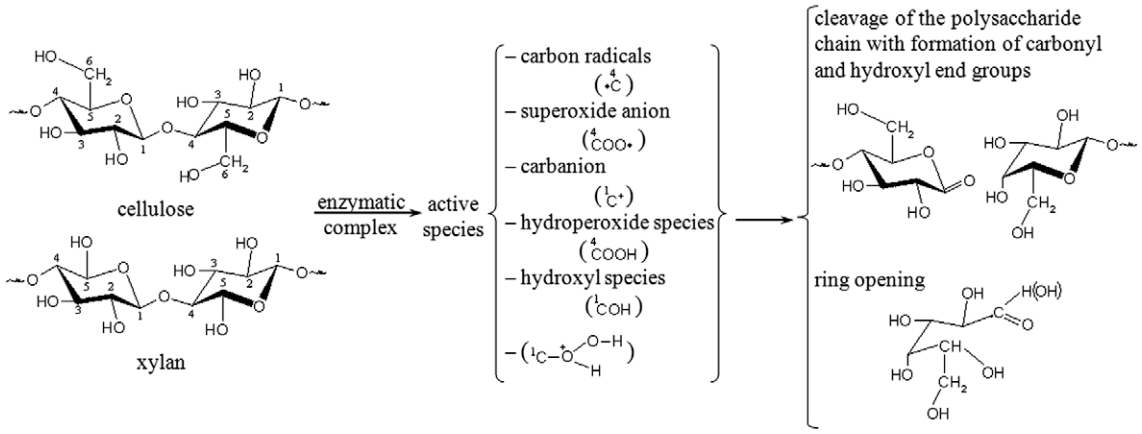

Fig. 12. Schematic representation of enzymatic degradation of carbohydrates.

time-dependent IR spectra of biodegraded lime wood combined with 2D-correlation analysis, and their second derivative analysis can provide detailed information about the modifications induced by fungi decay. 2D-correlation spectra were able to explore the structural changes in wood due to a variety of oxidoreductions, some of which resulting in cleavage of the polysaccharide chain. *T. viride* removed structural carbohydrate components selectively with formation of oxidized compounds and finally being formed small molecules or fragments containing functional groups. Also, values for ratios I_{1462}/I_{1511} and I_{1425}/I_{1511}, decreases during decay of 84 days, from 1.24 to 1.06 and from 0.74 to 0.62, respectively. This small decrease may be due to xylan decay, since both of peaks have a contribution from carbohydrates.

The crystallinity degrees of decayed wood samples are decreasing during exposure time to the fungus.

These results indicate an enzymatic oxidation and hydrolysis reactions on hemicelluloses and cellulose resulting oligomers and oxidized structures, and finally small fragments containing carboxyl or carbonyl groups are formed, which are lost or remain in wood structures.

References

Czarnecki, M. A. (1998). Interpretation of two-dimensional correlation spectra: Science or art? *Applied Spectroscopy, 52*, 1583–1590.

Eriksson, K. E. L., Blanchette, R. A., & Ander, P. (1990). *Microbial and enzymatic degradation of wood and wood components*. Berlin: Springer.

Faix, O. (1992). Fourier transform infrared spectroscopy. In S. Y. Lin & C. W. Dence (Eds.), *Methods in lignin chemistry* (pp. 83–109). Berlin: Springer.

Faix, O., Bremer, J., Schmidit, O., & Stevanovic, T. (1993). Monitoring of chemical changes in white-rot degraded beech wood by pyrolysis-gas chromatography and Fourier transform infrared spectroscopy. *Journal of Analytical Applied Pyrolysis, 21*, 147–162.

Ferraz, A. U., Baeza, J., Rodrigues, J., & Freer, J. (2000). Estimating chemical composition of biodegraded pine and eucalyptus by DRIFT spectroscopy and multivariate analysis. *Bioresource Technology, 74*, 201–212.

Goodell, J., & Jellison, J. (1998). The role of biological metal chelator in wood degradation and xenobiotic degradation. In A. Bruce & J. W. Palfreyman (Eds.), *Forest product biotechnology* (pp. 235–249). London: Taylor and Francis.

Goodell, B., Jellison, J., Liu, J., Daniel, G., Paszczynski, A., Fekete, F., et al. (1997). Low molecular weight chelators and phenolic compounds isolated from wood decay fungi and their role in fungal biodegradation of wood. *Journal of Biotechnology, 53*, 133–162.

Hammel, K. E., Kapich, A. N., Jensen, K. A., Jr., & Ryan, Z. C. (2000). Reactive oxygen species as agents of wood decay by fungi. *Enzyme and Microbial Technology, 30*, 445–453.

Hulleman, S. H. D., Van Hazendonk, J. M., & Van Dam, J. E. G. (1994). Determination of crystallinity in native cellulose from higher plants with diffuse reflectance Fourier transform infrared spectroscopy. *Carbohydrate Research, 261*, 163–172.

Ilharco, L. M., Garcia, A. R., Lopes da Silva, J., & Ferreira, L. F. V. (1997). Infrared approach to the study of adsorption on cellulose: Influence of cellulose crystallinity on the adsorption of benzophenone. *Langmuir, 13*, 4126–4132.

Kondo, T. (2005). Structure and functional versatility. In S. Dumitriu (Ed.), *Polysaccharides II* (pp. 69–98). New York: Marcel Dekker.

Korner, I., Faix, O., & Wienhaus, O. (1992). Attempts to determine the degradation of pine wood due to brown rot with the aid of FTIR spectroscopy. *Holz als Roh und Werkstoff, 50*, 363–367.

Kubo, S., & Kadla, J. F. (2005). Hydrogen bonding in lignin: A fourier transform infrared model compound study. *Biomacromolecules, 6*, 2815–2821.

Martinez, A. T., Camarero, S., Gutierrez, A., Bochini, P., & Galleti, G. C. (2001). Studies on wheat lignin degradation by *Pleurotus* species using analytical pyrolysis. *Journal of Analytical and Applied Pyrolysis, 58–59*, 401–411.

Moore, A. K., & Owen, N. L. (2001). Infrared spectroscopic studies of solid wood. *Applied Spectroscopy Reviews, 36*, 65–86.

Nishiyama, Y., Sugiyama, J., Chanzy, H., & Langan, P. (2003). Crystal structure and hydrogen bonding system in cellulose I_α from synchrotron X-ray and neutron fiber diffraction. *Journal of American Chemical Society, 125*, 14300–14306.

Noda, I. (1993). Generalized two-dimensional correlation method applied to infrared, Raman, and other types of spectroscopy. *Applied Spectroscopy, 47*, 1329–1336.

Pandey, K. K. (1999). A study of chemical structure of soft and hardwood polymers by FTIR spectroscopy. *Journal of Applied Polymer Science, 71*, 1969–1975.

Pandey, K. K., & Theagarajan, K. S. (1997). Analysis of wood surfaces by diffuse reflectance (DRIFT) and photoacoustic (PAS) Fourier transform infrared spectroscopic techniques. *Holz als Roh und Werkstoff, 55*, 383–390.

Perez, S., & Mazeau, K. (2005). Structure and functional versatility. In S. Dumitriu (Ed.), *Polysaccharides II* (pp. 41–68). New York: Marcel Dekker.

Pérez, J., Muñoz-Dorado, J., de la Rubia, T., & Martínez, J. (2002). Biodegradation and biological treatments of cellulose, hemicelluloses and lignin: An overview. *International Microbiology, 5*, 53–63.

Popescu, M. C. (2009). Contributions to optical characterization of some multicomponent polymeric blends. Ph.D. Thesis.

Popescu, C. M., Popescu, M. C., Singurel, Gh., Vasile, C., Argyropoulos, D. S., & Willfor, S. (2007). Spectral characterization of eucalyptus wood. *Applied Spectroscopy, 61*(11), 1168–1177.

Popescu, C. M., Vasile, C., Popescu, M. C., & Singurel, Gh. (2006). Degradation of lime wood painting supports. II. Spectral characterization. *Cellulose Chemistry and Technology, 40*(8), 649–658.

Rodrigues, J., Faix, O., & Pereira, H. (1998). Determination of lignin content of eucalyptus globules wood using FTIR spectroscopy. *Holzforschung, 52*, 46–50.

Schmidt, O., & Czeschlik, D. (2006). Wood cell wall degradation. In *Wood and tree fungi: Biology, damage, protection, and use* (pp. 87–106). Springer.

Schwanninger, M., Rodrigues, J. C., Pereira, H., & Hinterstoisser, B. (2004). Effects of short-time vibratory ball milling on the shape of FT-IR spectra of wood and cellulose. *Vibrational Spectroscopy, 36*, 23–40.

Struszczyk, H. (1986). Modification of lignins. III. Reaction of lignosulfonates with chlorophosphazenes. *Journal of Macromolecular Science A, 23*, 973–992.

Šturcová, A., His, I., Apperley, D. C., Sugiyama, J., & Jarvis, M. C. (2004). Structural details of crystalline cellulose from higher plants. *Biomacromolecules, 5*, 1333–1339.

Sugiyama, J., Persson, J., & Chanzy, H. (1991). Combined infrared and electron diffraction study of the polymorphism of native celluloses. *Macromolecules, 24*, 2461–2466.

Watanabe, A., Morita, S., & Ozaki, Y. (2006). Study on temperature-dependent changes in hydrogen bonds in cellulose Ib by infrared spectroscopy with perturbation–correlation moving-window two-dimensional correlation spectroscopy. *Biomacromolecules, 7*, 3164–3170.

Watanabe, A., Morita, S., & Ozaki, Y. (2007). Temperature-dependent changes in hydrogen bonds in cellulose Ia studied by infrared spectroscopy in combination with perturbation–correlation moving-window two-dimensional correlation spectroscopy: Comparison with cellulose Ib. *Biomacromolecules, 8*, 2969–2975.

Zabel, R. A., & Morell, J. J. (1992). *Wood microbiology decay and its prevention*. San Diego: Academic Press Inc.